Influence of indenter geometry on arcuate fold-and-thrust wedge: preliminary results of analogue modelling

Influencia de la geometría del indenter sobre el desarrollo de una cuña de pliegues y cabalgamientos arqueados: Resultados preliminares de modelos analógicos

A. Crespo-Blanc y A. González-Sánchez

Departamento de Geodinámica - IACT. Universidad de Granada - CSIC. C/Fuentenueva, s/n. 18071 Granada. acrespo@ugr.es

ABSTRACT

Analogue models, with sand and silicone, have simulated the progressive development of an arcuate fold-and-thrust belt around indenters of different geometry, which moved along a straight translation path. In the most external part of the model, the resulting geometry of the deformed wedge is roughly independent of the indenter form. Deformation affected only the frontal part of the indenter and the lateral deformation zone around the latter was very narrow.

Key words: *Analogue modelling, arcuate fold-and-thruts belt, indenter geometry, frictional and viscous substrate, sand, silicone.*

RESUMEN

Modelos analógicos con arena y silicona simularon el desarrollo progresivo de un cinturón arqueado de pliegues y cabalgamientos alrededor de un indenter *con formas variables y con una trayectoria recta. En la parte más externa del modelo, la geometría resultante de la cuña deformada no depende de la forma del* indenter*. La deformación afecta solo a la parte frontal del* indenter*, y la zona de deformación lateral alrededor del mismo es muy estrecha.*

Geogaceta, 37 (2005), 11-14
ISSN: 0213683X

Introduction

The development of arcuate fold-and-thrust belt developed in external zones of mountain range has been investigated through analogue modelling experiments. Among others, in such experiments, the two most important factors that control the non-cylindrism of the deformed wedge are the lateral variation of the substrate type (viscous or frictional, modelled by silicone or sand, respectively) in turn related with palaeogeography of the paleomargin in the studied natural case, (e.g. Corrado *et al.*, 1998; Luján *et al.*, 2003), and the indentation of a rigid backstop, in turn related with the geometry of the internal part of the orogen which push-from-behind the sedimentary rocks which will be incorporated to the deformed wedge (e.g. Likorish *et al.*, 2002 and references herein). In previously published models of this second type of modelling, the geometry of the indenters was unrealistic, with straight, rectangular boundaries (*op.cit.*).

In this paper, preliminary results deriving from sandbox analogue experiments are presented: non-cylindrical fold-and-thrust wedges have been generated around backstop of different geometry, in order to reproduce natural cases of the Betic external zones. A first group of experiments have been realized with sand, with a push-from-behind indenter, which moved along a straight translation path; they model arcuate deformed wedges of carbonate sedimentary rocks. An experiment with a backstop indenting in an undeformed wedge of sand with a silicone basal layer, which simulates Triassic evaporites, is also discussed. This permits to investigate the influence of the substrate on arcuate fold-and-thrust wedge development.

Model set up and experimental conditions

All the experiments were realized in the Analogue modelling Laboratory of the Geodynamic Department of the University of Granada. Dry, rounded quartz sand with a grain size varying between 0.2 and 0.3 mm, were used in a natural gravity field to simulate the Mohr-Coulomb behaviour of competent sedimentary rocks undergoing brittle deformation at shallow crustal levels (e.g. Davy and Cobbold, 1991). Coloured sand was used to provide horizontal passive markers within the undeformed experimental multilayer. The experiments were performed in a 60cm long and 50cm wide sandbox, floored by a drafting film sheet, and with a mobile, rigid indenter, 25cm width, situated in the rear side of the sandbox (Fig. 1).

In experiments constitued only by sand —that is with a frictional substrate—, this latter was confined by woodblocks and sieved above the sheet, until it reached 1.5cm height. A reference grid of 4 cm-sided squares was sieved onto the top layer of the sandpack. The indenter was pushed against the

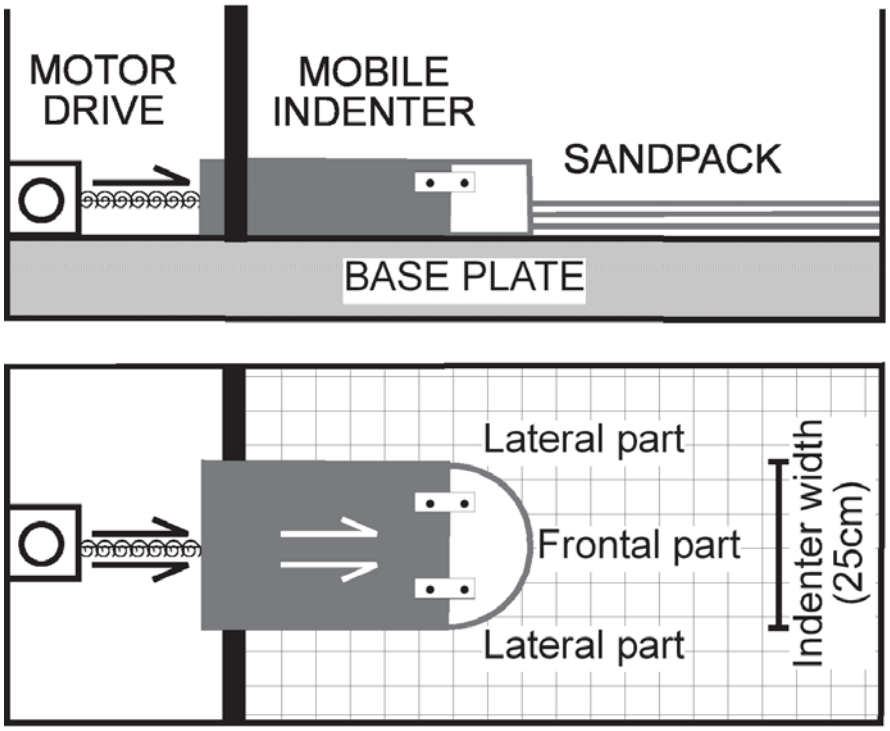

Fig. 1.- Simplified sketch of the experimental apparatus and model setting. The frontal part of the indenter, in white, is interchangeable.

Fig. 1.- Esquema simplificado del aparato y del modelo inicial. La parte frontal del* indenter, *en blanco, es intercambiable.

undeformed multilayer along an straight translation path, parallel to the lateral edge and at a constant rate of 10cm/hour (Fig. 1), which induced the growth of a Coulomb wedge in the sandpack. It will be referred as frontal and lateral parts of the models with reference to the indenter translation path (Fig. 1). The changing geometry was recorded by time lapse photography of the experiment plan. After completion, each model underwent serial sectioning parallel to the shortening direction. Total movement of the backstop was similar for all experiments (21 to 28cm). Four different indenter geometries have been used and its frontal part was rectangular, half-circular, half-elliptical (with a ratio value between axes of 0.5) and asymmetrical. The form of each indenter can be observed in figure 2.

In order to test the influence of the substrate on the resulting geometry, an experiment has been made with a viscous, silicone layer at the base of the sandpack. The viscous layer was 0.5cm high, the overlying sand layer 1.0cm and the asymmetrical indenter was used. The mechanical properties of the silicone putty (transparent Rhodosil Gum FB of Rhone-Poulenc) can be found in Brun and Fort (2004). The velocity of the screw moving the indenter was 0.75cm/hour, which corresponds to a natural velocity of 0.5 to 2cm/y according to the common scaling of such type of experiment (Weijermars and Schmeling, 1986).

Experimental results

Frictional substrate models

In all experiments with a frictional substrate, the shortening induced by the backstop indenting in the sand pack produce a typical Coulomb wedge in which the arcuate foreland-verging imbricates, rooted at the bottom of the sand pack, were accreted in a piggyback fashion (Fig. 2A to D, see also Fig. 5A). In map view, the general fold-and-thrust geometry of the deformed sand wedge corresponds with that of an arc that systematically developed during the initial stages of shortening. Indeed, the first thrusts which formed mimic the shape of the backstop, as illustrated by figure B1, which shows an intermediate stage of the experiment with the elliptic indenter. Then, when the wedge toe incorporated more material, the length of the most external arcuate thrust increased, and the width of the area affected by shortening

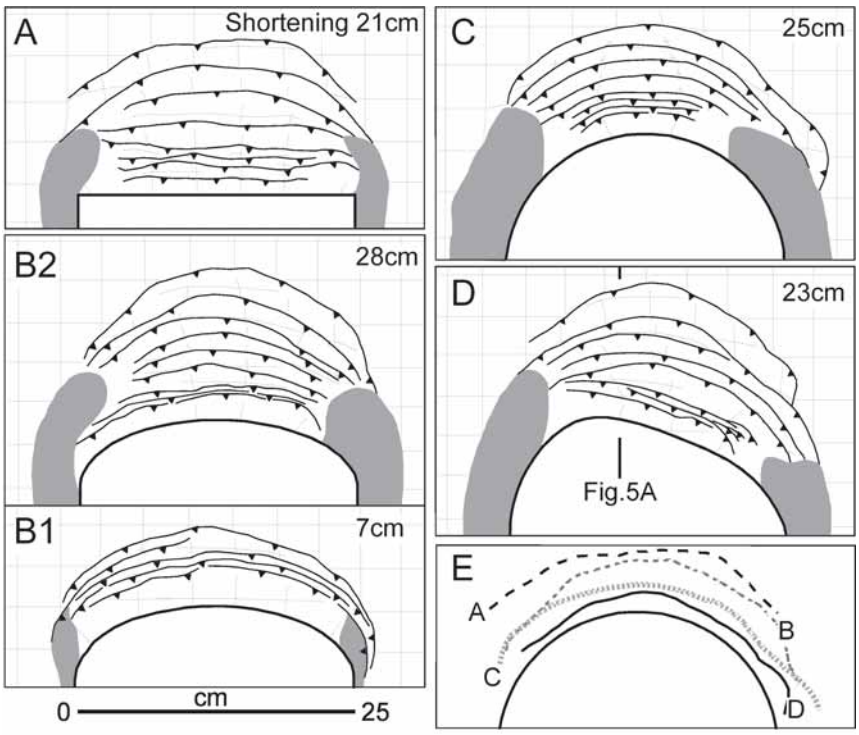

Fig. 2.- A to D: Line drawing after photographs of the final (A, B2, C, D) and intermediate (B1) geometry of sandbox experiments with various indenter forms. In grey, slumped sand. E: For comparison, the frontal thrust final geometry of the same models has been drawn in the same sketch, together with the circular indenter.

Fig. 2.- A a D: Dibujo a partir de las fotografías de la geometría final (A, B2, C, D) e intermedio (B1) de diversos experimentos con arena, en los que la forma del* indenter *varía. En gris, arena deslizada. E: Para comparar, se ha dibujado sobre el mismo esquema, la geometría de los cabalgamientos frontales de los mismos experimentos, junto con la forma del* indenter *circular.

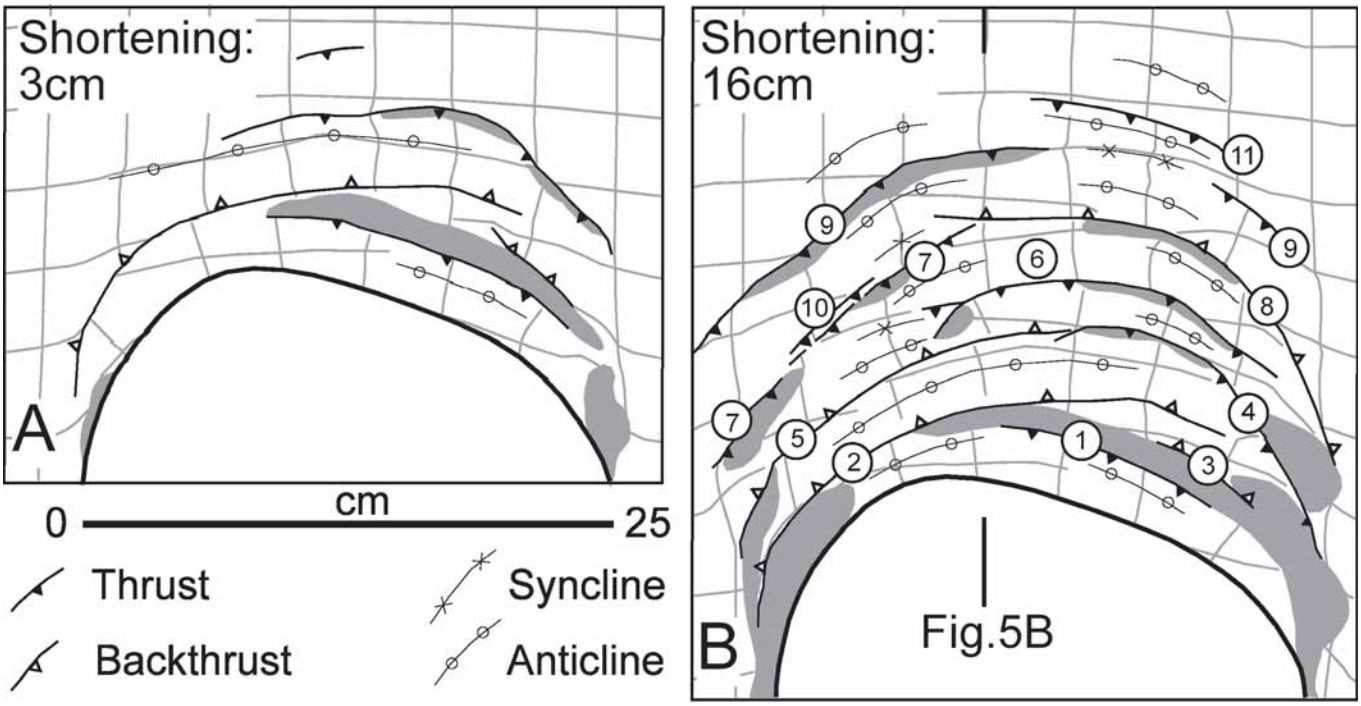

Fig. 3.- Line drawing after photographs of the intermediate (A) and final geometry (B) of the model composed by sand sieved over silicone, with the asymmetrical indenter. Numbers indicate the nucleation sequence of the faults.

Fig. 3.- Dibujo a partir de las fotografías de la geometría de un estadio intermedio (A) y final (B) del modelo compuesto por arena sobre silicona, con el* indenter *asimétrico. Los números indican la secuencia de nucleación de las fallas.

was larger than that of the backstop. Nevertheless, very quickly, this width stopped growing, and the lateral area of the deformed wedge was occupied by slumped areas (approximately 5cm on each lateral, that is a 20% of the indenter width) (Fig. 2A to D).

The resulting geometry of the wedge developed in front of the different indenters can be compared. Surprisingly, it can be observed that both the curvature and the form of the most external thrust are roughly independent of the indenter geometry and correspond approximately with a semicircle, slightly wider than the backstop (Fig. 2E). Indeed, around the semicircular indenter, the successive thrust formed almost parallel (Fig. 2C), meanwhile the thrusts that develop successively around the others indenters —rectangular, elliptical or asymmetrical— showed a more and more pronounced curvature until they reach a circular geometry (after the fifth or sixth thrust), which probably depends only of the indenter width.

Viscous substrate model

A drastic change of geometry with respect to the models previously described is observed in the model in which an asymmetrical indenter produced shortening in a sandpack sieved over a silicone layer (Fig. 3). Indeed, although an arcuate fold-and-thrust belt is still observed, the presence of a viscous substrate induced the development of backthrusts, as clearly pointed out in the oblique photograph of the experiment final stage (Fig. 4). A cross-section illustrates the structural characteristic of this wedge (Fig. 5B). Opposite-verging thrusts, rooted in the silicone, globally defining pop-up and pop-down structures, are associated with the folds whose axial traces are drawn in the map view of figure 3. When compared with a section of the model with the same indenter but formed only by sand (Fig. 5A), where a simple foreland-verging leading imbricate fan developed (Mulugeta, 1988; Liu *et al.*, 1992), the differences are outstanding. In particular, the topographic angle of the wedge developed over a frictional substrate is much higher than that of the wedged built over a viscous substrate, as in this latter, the vergence of the structures is not so clearly defined.

The sequence of nucleation of the thrusts and backthrusts is indicated by the numbers of figure 3B. The first thrust which develops is foreland-ward and mimics the backstop geometry. Then, a pair thrust-backthrust associated with folds, developed almost simultaneously when shortening increase in front of the indenter (Fig. 3A). The thrust are convex and the backthrust concave with respect to the indenter movement, and both type of structures draw an arcuate fold-and-thrust belt. It must be stressed that the thrust developed with an almost semi-circular geometry in the external part of the experiment —and not asymmetrical as the indenter— and that the deformed area is situated mainly in front of the indenter, as it is only slightly wider than this latter.

Discussion and conclusions

The sandbox experiments presented in this paper have modelled successfully the progressive development of an arcuate fold-and-thrust belt around indenters of different geometry, which moved along a simple, straight translation path. It is surprising to observe that for similar initial configuration of the experiments developed onto a frictional substrate, the resulting geometry of the most external structures is independent of the indenter form, and probably depends only of its width.

The described models are similar to the deformation style in natural cases of the external Betics, in particular the external Prebetic arc (see Fig. 4.9 of Vera

Fig. 4.- Oblique view of the final stage of the model composed by sand sieved over silicone.

Fig. 4.- Vista oblícua del estadio final del experimento compuesto por arena sobre una capa de silicona

Fig. 5.- Cross-sections cut parallel to the tectonic transport direction at the end of the experiment of the models with frictional (A) and viscous substrate (B). Locations in Fig. 2D and Fig. 3B, respectively.

Fig. 5.- Cortes paralelos a la dirección de transporte tectónico al final de los experimentos de los modelos con sustrato friccional (A) y viscoso (B). Localización de los cortes en las figuras 2D y 3B, respectivamente.

2003). Indeed, this arc, formed by a carbonate rock sequence, draws an almost perfect segment of circle around Alcaraz Sierra, although it must be stressed that in that case, the indenter is not so rigid, as the internal part of the arc is occupied by the internal Prebetic units, in turn formed by a stack of sedimentary rocks.

Our models failed to explain the distribution of the external units around the Gibraltar Arc (Flysch and Subbetic units, see figures 4.1 and 4.2 of Vera 2003), which completely surround the Alboran Domain internal zone, which in turn acted as a rigid indenter during a process of push-from-behind (Luján *et al.* 2003). Indeed, in the analogue models, deformation took place only in the frontal part of the indenter (as defined in Fig. 1). So, the deformed wedge is only slightly wider than the indenter. This occurred not only in the models with a frictional substrate but also in that with a viscous substrate, because the individual particule movement in the central part of the indenter is largely parallel with the movement of this latter; meanwhile, in the lateral part of the indenter, they only slightly deviate from parallelism. Consequently, a single translation path of the Alboran Domain, parallel with its lateral boundary, can not explain the variation of the tectonic transport direction observed in the Gibraltar Arc external zones, as this direction swings almost 140º from one branch to the other of the Arc (Crespo-Blanc and Campos, 2001): a multiphase indentation path, different for each branch of the Arc, or a much complex indenter geometry must be invoked.

Acknowledgments

This study was supported by Grant BTE2003-05057-CO2-01 (Spain). More results together with animations of thrust wedge development can be seen in http://www.ugr.es/~geodina/, the web page of the Analogue Modelling Laboratory of the Geodynamic Department (University of Granada).

References

Brun, J.P. y Fort, X. (2004). *Tectonophysics*, 382, 129-150.

Corrado, S., DiBucci, D., Naso, G. y Faccenna, C. (1998). *Tectonophysics*, 296, 437-453.

Crespo-Blanc, A. y Campos, J. (2001). *Journal of Structural Geology,* 23/10, 1615-1630.

Davy, P., y Cobbold, P. R. (1991). *Tectonophysics*, 188, 1-25.

Likorish, W.H., Ford, M., Bürgisser, J. y Cobbold, P.R. (2002). *Geological Society of America Bulletin*, 114/9, 1089-1107.

Liu, H., McClay, K.R. y Powell, D. (1992). En: *Thrust tectonics.* McClay (Ed.), Chapman and Hall: 71-81.

Luján, M., Storti, F., Balanyá, J.C., Crespo-Blanc, A. y Rossetti, F. (2003). *Journal of Structural Geology,* 25/6, 867-881.

Mulugeta, G. (1988). *Journal of Structural Geology,* 10, 847-859.

Vera, J.A. (2003). *Geología de España* SGE-IGME, 890p.

Weijermars, R. y Schmeling, H. (1986). *Physical of Earth Planetary Interiors*, 43, 316-330.